Immunomodulatory properties of umbilical cord blood-derived small extracellular vesicles and their therapeutic potential for inflammatory skin disorders

Sílvia C. Rodrigues (1,4), Renato M. S. Cardoso (1), Patricia C. Freire (1), Cláudia Gomes (1),

Filipe Duarte (1), Ricardo Neves (1-3), Joana Simões-Correia (1-3)

(1)   Exogenus Therapeutics, S.A., Cantanhede, Portugal

(2)   Center for Neurosciences and Cell Biology (CNC), University of Coimbra, Coimbra, Portugal

(3)   Institute for Interdisciplinary Research (3Is), University of Coimbra, Coimbra, Portugal

(4)   Doctoral Programme in Experimental Biology and Biomedicine (PDBEB), Institute for Interdisciplinary Research (IIIUC), CNC—Center for Neuroscience and Cell Biology, University of Coimbra., Coimbra, Portugal

Corresponding author: Joana Correia, Exogenus Therapeutics, S.A., Biocant Park, Cantanhede, Portugal; joana.correia@exogenus-t.com

SHORT TITLE

Bio-based immune modulation in skin disease

ABSTRACT

Umbilical cord blood (UCB) has long been seen as a rich source of naïve cells with strong regenerative potential, likely mediated by small extracellular vesicles (sEV). More recently, small extracellular vesicles (sEV), such as exosomes, have been shown to play essential roles in cell-to-cell communication, via the transport of numerous molecules, including small RNAs. Often explored for their potential as biomarkers, sEV are now known to have regenerative and immunomodulating characteristics, particularly if isolated from stem cell-rich tissues. In this study, we aim to characterize the immunomodulating properties of umbilical cord blood mononuclear cell sEV (herein referred as Exo-101), and explore their therapeutic potential for inflammatory skin diseases. Exo-101 was shown to shift macrophages toward an anti-inflammatory phenotype, which in turn exert paracrine effects on fibroblasts, despite previous inflammatory stimuli. Additionally, the incubation of PBMC with Exo-101 resulted in an reduction of total $CD4^+$ and $CD8^+$ T-cell proliferation and cytokine release, while specifically supporting the development of regulatory T-cells (Treg), by influencing FOXP3 expression. In a 3D model of psoriatic skin, Exo-101 reduced the expression of inflammatory and psoriatic markers IL-6, IL-8, CXCL10, COX-2, S100A7 and DEFB4. *In vivo*, Exo-101 significantly prevented or reversed acanthosis in imiquimod-induced psoriasis, and tendentially increased the number of Treg in skin, without having an overall impact on disease burden. This work provides evidence for the anti-inflammatory and tolerogenic effect of Exo-101, which may be harnessed for the treatment of Th17-driven inflammatory skin diseases, such as psoriasis.

INTRODUCTION

Virtually every living cell releases extracellular vesicles (EV), which can be classified based on size and marker expression. One of the smallest known groups of EV, exosomes, have a diameter typically ranging from 30 to 100 nm and originate from endosomes (Raposo and Stoorvogel 2013). Composed of lipids, proteins and nucleic acids, these ubiquitous vesicles are thought to be involved in multiple diseases, including inflammatory and autoimmune skin conditions (Wang et al. 2019). Due to their physical characteristics, which allow them to carry molecules across long distances, EV are often explored for their potential as biomarkers (McBride et al. 2017; Wang et al. 2020). Physiologically, small EV (sEV), such as exosomes, are key mediators of cellular communication, namely through microRNAs (van Niel et al. 2018). Hence, depending on the producing cell, sEV may have modulating characteristics, which can potentially be harnessed for therapeutic purposes. In fact, these naturally-produced vesicles are currently explored for the treatment of several conditions, including wound healing (Henriques-Antunes et al. 2019) and autoimmune diseases (Bai et al. 2017; Kim et al. 2005; Ma et al. 2019). Their use replaces cell therapies (Phinney and Pittenger 2017; Di Trapani et al. 2016), while conferring advantages, namely concerning handling and formulation.

Umbilical cord blood (UCB) is a rich source of stem cells and immature T-cells (Harris et al. 1992) with potent suppressive ability (Godfrey et al. 2005). The collection of UCB, commonly seen as medical waste, is non-invasive and has limited ethical concerns. We have previously shown that sEV from UCB mononuclear cells (MNC) accelerate the healing of diabetic wounds (Henriques-Antunes et al. 2019). In this study, we characterize the immunomodulating properties of UCB-MNC-derived sEV, Exo-101, and explore their potential in the treatment of psoriasis symptoms.

3

RESULTS

Exo-101 has anti-inflammatory and tolerogenic effects, modulating different immune players directly and indirectly

While exploring the therapeutic potential of Exo-101 for chronic wound healing (Cardoso et al. 2021; Henriques-Antunes et al. 2019), we found differences in the immunological profile of treated versus control skin. Namely, 194 genes associated with immune system processes or inflammatory responses, corresponding to about 16% of all measured genes, were differentially expressed between the two groups of animals (Figure S1). Based on these results and on existing literature, we performed a series of *in vitro* proof-of-concept experiments to determine the nature and strength of Exo-101's immunomodulatory effect.

In line with studies using sEV from different sources (Cao et al. 2019; Hu et al. 2020), Exo-101 promotes the differentiation of macrophages into an anti-inflammatory M2, rather than a pro-inflammatory M1 phenotype (Figure 1). This effect is present both in unstimulated (Figure 1a-c) and LPS-stimulated macrophages (Figure 1d-f) and correlates with the *de novo* synthesis and release of inflammatory mediators (Figure 1a-l). Specifically, Exo-101 administration significantly decreases the level of *IFNG*, *IL1B*, *PTSG2* and *TNFA* mRNA in macrophages, as well as the release of TNFα and CCL20 proteins. These data strongly indicate that Exo-101 plays a direct role in macrophage regulation, having an anti-inflammatory effect, even in the context of an acute pro-inflammatory stimulus.

At the local level, Exo-101 directly promotes the proliferation of dermal fibroblasts (Figure 1m-n). Interestingly, the incubation of fibroblasts with conditioned medium from Exo-101-stimulated macrophages likewise modulates cell proliferation, as well as chemokine synthesis, with a more pronounced effect when compared to direct Exo-101 stimulation (Figure 1o). These results suggest that, while Exo-101 does act directly on target skin cells, its effects

are likely reinforced by indirect mechanisms, depending on neighboring immune cell populations, such as macrophages.

To evaluate the response of T-cells to Exo-101 stimulation, in a physiological context, whole human PBMC were incubated for 6 days with a single dose of 1×10^{10} vesicles/mL, following activation with α-CD3/-CD28. Exo-101 significantly reduced the proliferation of total, CD4^{+} and CD8^{+} T-cells, as well as the intracellular content of IFNγ in each of these populations (Figure 2a-f). The release of TNFα and CCL20 by total PBMCs was also significantly decreased (Figure 2g,h). Notably, after two days of treatment, Exo-101 modulated the expression of population-specific transcription factors in CD4^{+} T-cells, with a trend towards the reduction of GATA-3, a significant decrease in T-bet and RORγt, and a significant increase in Foxp3 mRNA (Figure 2i-l). This effect was still visible after 6 days of treatment, for RORγt and Foxp3 expression.

To validate the differences in transcriptional regulation, we determined the populational T-cell changes by flow cytometry. As expected, Exo-101 treatment promoted the differentiation into regulatory T-cells (Treg), while inhibiting effector populations (Figure 2m-o). In this experiment, Tregs were defined as CD4^{+}CD25^{+}CD127^{-} cells, and the results were confirmed using a gating strategy based on the expression of the transcription factor Foxp3 (Figure S2). Importantly, Exo-101's effect was shown to be as powerful as IL-2 for the induction of Treg (Figure 2m and S2).

Exo-101 reduces the expression of psoriasis markers, in an *in vitro* 3D model

Considering the results from Figure 2, which evidenced an immunomodulatory effect of Exo-101, particularly focused on the Th17 and Treg response, we decided to evaluate the therapeutic benefit of Exo-101 in psoriasis. Using an in vitro 3D model of reconstructed human epidermis, engineered to be histologically and metabolically similar to psoriatic skin, we show

that Exo-101 treatment significantly reduced the expression of the inflammatory mediators IL-6, IL-8, CXCL10 and COX-2, and had a tendential effect on *IFNG* and *TNFA* mRNA (Figure 3a-h). Moreover, the expression of psoriasin (S100A7) and beta-defensin-2 (DEFB4), two psoriasis-associated antimicrobial peptides, was also significantly decreased (Figure 3i,j).

Exo-101 shows a modest effect in imiquimod-induced psoriasis, regulating keratinocyte proliferation and T-cell homeostasis

Application of imiquimod, a TLR7 agonist, to mouse's skin leads to the development of psoriatic features, such as, among others, epidermal thickening, erythema, inflammatory cell infiltration and epidermal expression of IL-17 (van der Fits et al. 2009). Daily topical treatment with Exo-101, dissolved in a slow-release hydrogel and applied one hour after imiquimod, did not significantly ameliorate macroscopic psoriasis-like features, when compared to hydrogel alone (Figure 4a,b). However, Exo-101 was significantly superior to hydrogel at reducing acanthosis, as seen by microphotographs (Figure 4c,d). The expression of the inflammatory markers TNFα, IFNγ, IL-17A, CCL20 and CXCL1, albeit significantly reduced when compared to the imiquimod control, was similar between the two groups receiving hydrogel, with or without Exo-101 (Figure 4e-i). When comparing the three treatment groups, there were no major changes in the skin infiltration of most inflammatory cells, including neutrophils, macrophages, total T-cells, γδ T-cells and total CD4$^+$ T-cells (Figure 4j-k and S3). CD8$^+$ T-cells were slightly reduced in Exo-101-treated animals compared to the skin of mice receiving only hydrogel (Figure 4l). Furthermore, Exo-101 tendentially increased the number of Treg in the skin of imiquimod-treated mice (Figure 4m), a finding that is consistent with gene expression data from diabetic mice with chronic skin wounds (Figure S4)(Cardoso et al. 2021; Henriques-Antunes et al. 2019). These findings indicate that, in a context of psoriasis, Exo-101 improves certain pathological features, possibly through a mechanism that involves

both local and immune cells, but did not significantly reduce the overall disease burden in this model.

DISCUSSION

Over the last years, sEV have been explored for their potential as cell-free immunomodulatory and regenerative agents. Indeed, unmodified or engineered sEV were shown to have therapeutic potential across multiple conditions, including cancer (Yuan et al. 2019), inflammatory lung diseases (Zhang et al. 2018; Zhu et al. 2014) and autoimmunity (Lai et al. 2019). Here, we explore the mechanism of action of sEV isolated from UCB-MNC, Exo-101, and evaluate their effect in psoriasis models.

In vitro, Exo-101 exhibits anti-inflammatory properties, affecting macrophage differentiation and cytokine production. These results are consistent with previous findings using sEV isolated from bone marrow (Cao et al. 2019) or cord blood (Hu et al. 2020). We also show that the presence of Exo-101-induced M2 macrophages has a down-stream effect on neighboring cells, such as skin fibroblasts, reducing their response to an inflammatory trigger. Moreover, Exo-101 strongly inhibited cell proliferation and cytokine production by LPS-stimulated total $CD4^+$ and $CD8^+$ T-cells, consistent with previous reports (Del Fattore et al. 2015; Di Trapani et al. 2016). This outcome is possibly due to an effect on T-cell differentiation, given that Exo-101 promotes a shift from a Th1 or Th17 into a Treg phenotype. Notably, Exo-101 stimulus was shown to be as effective as IL-2 in promoting Treg development.

Our *in vitro* findings evidenced a potential mechanism of action for Exo-101, responsible for a shift in the expression of transcription factors, which favor Treg differentiation and concomitantly silence Th17 signaling. Biologics targeting the Th17 axis (α-IL-17 and α-IL-23) have been proved to be clinically effective in ameliorating psoriasis symptoms (Gordon et al. 2018; Krueger et al. 2019; Papp et al. 2018). Additionally, previous reports suggest that Treg,

a typically tolerogenic cell population, play a crucial role the maintenance of skin homeostasis. Treg-deficient animals present an exacerbated response to imiquimod (Hartwig et al. 2018) and Treg from psoriatic patients display an impaired suppressive function (Sugiyama et al. 2005). Hence, we hypothesized that Exo-101's profile could be therapeutically beneficial in psoriasis. To test this, we employed a model of reconstructed human epidermis, composed of keratinocytes in various stages of differentiation, and pre-treated to display psoriasis-like inflammatory features. Exo-101 treatment significantly reduced the expression of psoriasis-associated molecules, including IL-6 and IL-8, as well as antimicrobial peptides S100A7 and DEFB4, thereby supporting its therapeutic potential for this disease.

In order to test Exo-101's effect *in vivo*, we first designed a micelle-rich hydrogel that solidifies at normal body temperature, thus reducing product loss when applied to the skin. Psoriasis-like symptoms were induced by topical applications of imiquimod, and hydrogel was applied one hour later, alone or containing Exo-101 vesicles. In this *in vivo* model, Exo-101 proved superior to hydrogel in reducing or preventing keratinocyte hyperproliferation, as measured by epidermal thickness. Yet, there were no significant differences in the disease scores, mRNA expression and cellular profile between the two treatment groups. While it is possible that the application of hydrogel alone strongly improves psoriatic symptoms, the results observed are better explained by the possible trapping of imiquimod molecules in hydrogel micelles, therefore preventing full symptom development. An alternative experimental setting would either allow for a longer time interval between imiquimod and test treatment applications and/or require the increase of imiquimod dosage. Nevertheless, in line with previous *in vitro* data, Exo-101 had a positive effect on keratinocytes and was tendentially stronger than hydrogel alone in shifting skin cellular infiltrates toward a tolerogenic profile. Importantly, gene expression data from chronic wounds support the increase in Treg differentiation following Exo-101 treatment. Given the incomplete therapeutic response of imiquimod-treated

animals to Exo-101, it is plausible that Exo-101 could act as an adjuvant treatment, in combination with standard therapies, such as anti-IL-17A or anti-IL23. This strategy would not only target immune-driven disease pathways, but also simultaneously stimulate repair mechanisms in the skin.

In conclusion, we show that Exo-101 decreases inflammation by targeting different cell populations, such keratinocytes, fibroblasts and macrophages, and by modulating T-cell differentiation and cytokine production. These findings warrant further proof-of-concept studies on the therapeutic potential of Exo-101 in inflammatory skin conditions, in particular, diseases thought to benefit from Th17/Treg-targeting.

MATERIALS AND METHODS

UCB collection, testing and data protection

Human UCB samples and relevant donor information were collected following signed informed consent, under approval of the Portuguese National Data Protection Committee and the ethics committees from five Portuguese hospitals, according to local legislation and following the principles of the Declaration of Helsinki. UCB processing, including microbiological testing, and storage were performed by an accredited biobank (Stemlab, S.A, Cantanhede, Portugal).

Cell culture

UCB-MNC

Isolated UCB-MNC were cultured under 0.5% O_2, for 18 hours, at a density of 2 million cells/mL in serum-free cell culture medium (Lonza AG, Basel, Switzerland) supplemented with 0.5 μg/mL FMS-like tyrosine kinase-3 (Peprotech, London, UK) and 0.5 μg/mL stem-cell factor (Peprotech, London, UK).

THP-1-derived macrophages

THP-1 cells (ATCC, Manassas, VA) were grown for 72 hours in the presence 25 nM PMA (Sigma, St. Louis, MO). THP-1-derived macrophages were then stimulated for 24 hours with 1 µg/mL LPS (Sigma, St. Louis, MO), followed by a 24-hour incubation with 1×10^{10} particles/mL Exo-101, when indicated.

Dermal fibroblasts

Normal human dermal fibroblasts were kept in Fibroblast Basal Medium, supplemented with Fibroblast Growth Kit Serum-Free, Phenol Red and Penicillin-Streptomycin-Amphotericin B Solution (ATCC, Manassas, VA). When appropriate, cells were counted after Hoescht staining (VWR International, Radnor, PA).

PBMC

Fresh human PBMC samples were isolated from volunteer donors, following informed consent, by density gradient centrifugation (Stemcell Technologies, Vancouver, Canada). For T-cell experiments, 2×10^5 cells/well were activated with PMA (Sigma, St. Louis, MO), anti-CD3/-CD28 (see Table 2) or LPS (Sigma, St. Louis, MO), as indicated, followed by a single dose of Exo-101 at 1×10^{10} particles/mL.

Exo-101 isolation

UCB-MNC culture media were subjected to an optimized isolation process, combining ultrafiltration and size exclusion chromatography (Cardoso et al. 2021). The resulting vesicles were characterized by transmission electron microscopy, flow cytometry, mass spectrometry for protein and lipid composition, RNA sequencing and nanoparticle tracking analysis, and found to be rich in CD63 and smaller than 200 nm (Cardoso et al. 2021).

Gene expression

RNA was extracted with RNeasy Mini Kit (Qiagen, Hilden, Germany) and analyzed with total RNA chips in Bioanalyzer 2100 (Agilent Technologies, Santa Clara, CA). SuperScript™ IV VILO™ Master Mix (ThermoFisher Scientific, Waltham, MA) was used for reverse transcription and gene expression was detected by qPCR, using the primer pairs in Table 1.

Table 1: Human and mouse primer sequences for qPCR

Target gene	Forward sequence	Reverse sequence
Human		
CXCL1	AGGGAATTCACCCCAAGAAC	ACTATGGGGGATGCAGGATT
CXCL10	TTCAAGGAGTACCTCTCTCTAG	CTGGATTCAGACATCTCTTCTC
DEFB4	ATCAGCCATGAGGGTCTTGT	GAGACCACAGGTGCCAATTT
FOXP3	GCTTCATCTGTGGCATCATC	TGGAGGAACTCTGGGAATGT
GATA3	CGCCTGCGGGCTCTATC	CCTTCGCTTGGGCTTAATGA
IFNG	GGTAACTGACTTGAATGTCC	TTTTCGCTTCCCTGTTTTAG
IL1B	CTAAACAGATGAAGTGCTCC	GGTCATTCTCCTGGAAGG
IL6	GGTACATCCTCGACGGCATCT	GT GCCTCTTTGCTGCTTTCAC
IL8	GTTTTTGAAGAGGGCTGAG	TTTGCTTGAAGTTTCACTGG
PTGS2	ATCTACCCTCCTCAAGTCCC	TACCAGAAGGGCAGGATACAG
RORC	TGGACCACCCCCTGCTGAGAA	CTTCAATTTGTGTTCTCATGACT
S100A7	CCAAACACACACATCTCACTCA	TCAGCTTGAGTGTTGCTCATC
TBX21	GATGTTTGTGGACGTGGTCTTG	CTTTCCACACTGCACCCACTT
TNFA	AGGCAGTCAGATCATCTTC	TTATCTCTCAGCTCCACG
Mouse		
CCL20	ACTGTTGCCTCTCGTACATACA	GAGGAGGTTCACAGCCCTTTT

CXCL1	GCTTGAAGGTGTTGCCCTCAG	AGAAGCCAGCGTTCACCAGAC
FOXP3	CACCCAGGAAAGACAGCAACC	GCAAGAGCTCTTGTCCATTGA
IFNG	CGGCACAGTCATTGAAAGCCTA	GTTGCTGATGGCCTGATTGTC
IL17A	TTTAACTCCCTTGGCGCAAAA	CTTTCCCTCCGCATTGACAC
TNFA	GTTCTATGGCCCAGACCCTCAC	GGCACCACTAGTTGGTTGTCTTTG

Protein quantification and flow cytometry (human)

TNFα and CCL20 were measured by ELISA (BioLegend, San Diego, CA). M1 macrophages were defined as CD14$^-$CD68$^+$CD86$^+$, and M2 macrophages as CD14$^-$CD68$^+$CD163$^+$ by flow cytometry. Tregs were defined as CD4$^+$CD25$^+$CD127$^-$ cells and the results were confirmed using a gating strategy based on the expression of the transcription factor *FOXP3* (Figure S2). Foxp3 expression was analyzed by flow cytometry using the Foxp3/Transcription Factor Staining Buffer Set (eBioscience, San Diego, CA). Whenever mentioned, IL-2 was used as a positive control for Treg development. Antibody details can be found in Table 2.

Table 2: Human and mouse antibodies for flow cytometry

Target	Clone	Manufacturer
Anti-human antibodies		
CD14	M5E2	BD Biosciences, San Jose, CA
CD163	GHI/61	BD Biosciences, San Jose, CA
CD28	CD28.2	BioLegend, San Diego, CA
CD3	OKT3	BioLegend, San Diego, CA
CD68	Y1/82A	BD Biosciences, San Jose, CA
CD86	FUN-1	BD Biosciences, San Jose, CA
IL-2	MQ1-17H12	BioLegend, San Diego, CA

Anti-mouse antibodies		
CD11b	M1/70	BD Biosciences, San Jose, CA
CD11c	HL3	BD Biosciences, San Jose, CA
CD16/CD32	2.4G2	Tonbo Biosciences, San Diego, CA
CD25	PC61.5	eBioscience, San Diego, CA
CD3e	145-2C11	BD Biosciences, San Jose, CA
CD4	RM4-5	BD Biosciences, San Jose, CA
CD45.2	104	eBioscience, San Diego, CA
CD62L	MEL-14	BD Biosciences, San Jose, CA
CD8	53-6.7	BD Biosciences, San Jose, CA
Ly6C	AL-21	BD Biosciences, San Jose, CA
Ly6G	1A8	BD Biosciences, San Jose, CA
TCR γ/δ	GL3	BioLegend, San Diego, CA
TCR α/β	GL2	BioLegend, San Diego, CA

Reconstructed psoriatic human epidermis

The 3D model of "psoriasis-like" human epidermis (Sterlab, Vallauris, France) was used according to the manufacturer's instructions. Briefly, epidermal inserts were placed in a 12-well feeder-plate and allowed to equilibrate in the supplied culture medium for one day at 37ºC and 5% CO_2, before treatment with 1×10^{10} particles/mL Exo-101, twice a day for 5 consecutive days.

Exo-101 formulation for *in vivo* topical use

Exo-101 is produced as a lyophilized powder. For *in vivo* experiments, Exo-101 was dissolved in a micellar hydrogel, which solidifies at body temperature, thereby reducing product loss when applied to the skin and allowing for a slow release of Exo-101 particles (not shown).

Imiquimod-induced psoriasis

Animal experiments were approved by the ethical committee of the Spanish National Cardiovascular Research Center, and performed according to national and European regulations, respecting animal welfare guidelines and the 3R's rule. 8-12-week-old C57BL/6 mice received daily applications of imiquimod (3M, Saint Paul, MN) on their shaved backs, for six consecutive days. One hour after every imiquimod application, $3x10^9$ particles/cm^2 Exo-101 dissolved in hydrogel were delivered topically. Epidermal thickness was measured on H&E-stained samples, using the software NanoZoomer Digital Pathology NDP.view2 (Hamamatsu Photonics, Hamamatsu, Japan), from stratum basale to stratum granulosum, averaging 5 measurements per section, for a total of 20 data points per animal. For flow cytometry, skin was digested with 0.25 mg/mL Liberase (Roche, Basel, Switzerland) in serum-free RPMI, for 60 min at 37ºC. Skin cell suspensions were stained with fluorescently-labelled antibodies, following Fc Block (Table 2). Absolute cell counts were performed using Trucount tubes (BD Biosciences, San Jose, CA). RNA analyses were performed as described above.

Statistical analyses

Data analyses were performed with Prism 6 (GraphPad Software, San Diego, CA). Unpaired t-tests or one-way ANOVA were employed whenever appropriate ($p < 0.05$).

DATA AVAILABILITY

For any data or certificate requests, please contact Exogenus Therapeutics, S.A., at team@exogenus-t.com.

CONFLICT OF INTEREST

S.C.R., P.C.F., R.M.S.C. and J.S-C. are or were employees of Exogenus Therapeutics, SA and R.N. and J.S-C. are Exogenus Therapeutics' co-founders and shareholders. R.M.S.C. and J.S-C. are inventors of the patent PCT/IB2017/000412 (use of umbilical cord blood derived exosomes for tissue repair) and R.M.S.C., S.C.R., and J.S-C. are inventors of the patent PCT/IB2019/058462 (compositions comprising small extracellular vesicles derived from umbilical cord blood mononuclear cells with anti-inflammatory and immunomodulatory properties), currently explored by Exogenus Therapeutics, SA. Financial interest is claimed by Exogenus Therapeutics, S.A., which holds a license (PCT/IB2017/000412) and a patent related to this work (PCT/IB2019/058462). The other authors declared no additional conflicts of interest.

ACKNOWLEDGMENTS

REFERENCES

Bai L, Shao H, Wang H, Zhang Z, Su C, Dong L, et al. Effects of Mesenchymal Stem Cell-Derived Exosomes on Experimental Autoimmune Uveitis. Sci. Rep. 2017;7(1):4323

Cao L, Xu H, Wang G, Liu M, Tian D, Yuan Z. Extracellular vesicles derived from bone marrow mesenchymal stem cells attenuate dextran sodium sulfate-induced ulcerative colitis by promoting M2 macrophage polarization. Int. Immunopharmacol. Netherlands; 2019;72:264–74

Cardoso RMS, Rodrigues SC, Gomes CF, Duarte F V, Romao M, Leal EC, et al. Development of an optimized and scalable method for isolation of umbilical cord blood-derived small extracellular vesicles for future clinical use. Stem Cells Transl. Med. John Wiley & Sons, Ltd; 2021;n/a(n/a) Available from: https://doi.org/10.1002/sctm.20-0376

Del Fattore A, Luciano R, Pascucci L, Goffredo BM, Giorda E, Scapaticci M, et al. Immunoregulatory Effects of Mesenchymal Stem Cell-Derived Extracellular Vesicles on T Lymphocytes. Cell Transplant. United States; 2015;24(12):2615–27

van der Fits L, Mourits S, Voerman JSA, Kant M, Boon L, Laman JD, et al. Imiquimod-Induced Psoriasis-Like Skin Inflammation in Mice Is Mediated via the IL-23/IL-17 Axis. J. Immunol. 2009;182(9):5836 LP – 5845 Available from: http://www.jimmunol.org/content/182/9/5836.abstract

Godfrey WR, Spoden DJ, Ge YG, Baker SR, Liu B, Levine BL, et al. Cord blood CD4(+)CD25(+)-derived T regulatory cell lines express FoxP3 protein and manifest potent suppressor function. Blood. United States; 2005;105(2):750–8

Gordon KB, Strober B, Lebwohl M, Augustin M, Blauvelt A, Poulin Y, et al. Efficacy and safety of risankizumab in moderate-to-severe plaque psoriasis (UltIMMa-1 and UltIMMa-2): results from two double-blind, randomised, placebo-controlled and ustekinumab-controlled phase 3 trials. Lancet. Elsevier; 2018;392(10148):650–61 Available from: https://doi.org/10.1016/S0140-6736(18)31713-6

Harris DT, Schumacher MJ, Locascio J, Besencon FJ, Olson GB, DeLuca D, et al. Phenotypic and functional immaturity of human umbilical cord blood T lymphocytes. Proc.

Natl. Acad. Sci. 1992;89(21):10006 LP – 10010 Available from:

http://www.pnas.org/content/89/21/10006.abstract

Hartwig T, Zwicky P, Schreiner B, Yawalkar N, Cheng P, Navarini A, et al. Regulatory T Cells Restrain Pathogenic T Helper Cells during Skin Inflammation. Cell Rep. United States; 2018;25(13):3564-3572.e4

Henriques-Antunes H, Cardoso RMS, Zonari A, Correia J, Leal EC, Jiménez-Balsa A, et al. The Kinetics of Small Extracellular Vesicle Delivery Impacts Skin Tissue Regeneration. ACS Nano. United States; 2019;13(8):8694–707

Hu W, Song X, Yu H, Sun J, Zhao Y. Released Exosomes Contribute to the Immune Modulation of Cord Blood-Derived Stem Cells [Internet]. Front. Immunol. . 2020. p. 165 Available from: https://www.frontiersin.org/article/10.3389/fimmu.2020.00165

Kim S-H, Lechman ER, Bianco N, Menon R, Keravala A, Nash J, et al. Exosomes derived from IL-10-treated dendritic cells can suppress inflammation and collagen-induced arthritis. J. Immunol. United States; 2005;174(10):6440–8

Krueger JG, Wharton KAJ, Schlitt T, Suprun M, Torene RI, Jiang X, et al. IL-17A inhibition by secukinumab induces early clinical, histopathologic, and molecular resolution of psoriasis. J. Allergy Clin. Immunol. United States; 2019;144(3):750–63

Lai P, Weng J, Guo L, Chen X, Du X. Novel insights into MSC-EVs therapy for immune diseases. Biomark. Res. 2019;7(1):6 Available from: https://doi.org/10.1186/s40364-019-0156-0

Ma D, Xu K, Zhang G, Liu Y, Gao J, Tian M, et al. Immunomodulatory effect of human umbilical cord mesenchymal stem cells on T lymphocytes in rheumatoid arthritis. Int. Immunopharmacol. Netherlands; 2019;74:105687

McBride JD, Rodriguez-Menocal L, Badiavas E V. Extracellular Vesicles as Biomarkers and Therapeutics in Dermatology: A Focus on Exosomes. J. Invest. Dermatol.

2017;137(8):1622–9 Available from:

http://www.sciencedirect.com/science/article/pii/S0022202X17314872

van Niel G, D'Angelo G, Raposo G. Shedding light on the cell biology of extracellular vesicles. Nat. Rev. Mol. Cell Biol. England; 2018;19(4):213–28

Papp KA, Merola JF, Gottlieb AB, Griffiths CEM, Cross N, Peterson L, et al. Dual neutralization of both interleukin 17A and interleukin 17F with bimekizumab in patients with psoriasis: Results from BE ABLE 1, a 12-week randomized, double-blinded, placebo-controlled phase 2b trial. J. Am. Acad. Dermatol. United States; 2018;79(2):277-286.e10

Phinney DG, Pittenger MF. Concise Review: MSC-Derived Exosomes for Cell-Free Therapy. Stem Cells. United States; 2017;35(4):851–8

Raposo G, Stoorvogel W. Extracellular vesicles: exosomes, microvesicles, and friends. J. Cell Biol. The Rockefeller University Press; 2013;200(4):373–83 Available from: https://pubmed.ncbi.nlm.nih.gov/23420871

Sugiyama H, Gyulai R, Toichi E, Garaczi E, Shimada S, Stevens SR, et al. Dysfunctional blood and target tissue CD4+CD25high regulatory T cells in psoriasis: mechanism underlying unrestrained pathogenic effector T cell proliferation. J. Immunol. 2005;174(1):164–73

Di Trapani M, Bassi G, Midolo M, Gatti A, Takam Kamga P, Cassaro A, et al. Differential and transferable modulatory effects of mesenchymal stromal cell-derived extracellular vesicles on T, B and NK cell functions. Sci. Rep. 2016;6(1):24120 Available from: https://doi.org/10.1038/srep24120

Wang W-M, Wu C, Jin H-Z. Exosomes in chronic inflammatory skin diseases and skin tumors. Exp. Dermatol. John Wiley & Sons, Ltd; 2019;28(3):213–8 Available from: https://doi.org/10.1111/exd.13857

Wang Z-Y, Yan B-X, Zhou Y, Chen X-Y, Zhang J, Cai S-Q, et al. miRNA Profiling of

Extracellular Vesicles Reveals Biomarkers for Psoriasis. J. Invest. Dermatol. Elsevier; 2020;

Available from: https://doi.org/10.1016/j.jid.2020.04.021

Yuan L, Liu Y, Qu Y, Liu L, Li H. Exosomes Derived From MicroRNA-148b-3p-

Overexpressing Human Umbilical Cord Mesenchymal Stem Cells Restrain Breast Cancer

Progression   [Internet]. Front. Oncol. . 2019. p. 1076 Available from:

https://www.frontiersin.org/article/10.3389/fonc.2019.01076

Zhang D, Lee H, Wang X, Rai A, Groot M, Jin Y. Exosome-Mediated Small RNA Delivery:

A Novel Therapeutic Approach for Inflammatory Lung Responses. Mol. Ther. Elsevier;

2018;26(9):2119–30 Available from: https://doi.org/10.1016/j.ymthe.2018.06.007

Zhu Y-G, Feng X-M, Abbott J, Fang X-H, Hao Q, Monsel A, et al. Human mesenchymal

stem cell microvesicles for treatment of Escherichia coli endotoxin-induced acute lung injury

in mice. Stem Cells. 2014;32(1):116–25 Available from:

https://pubmed.ncbi.nlm.nih.gov/23939814

FIGURES LEGENDS

Figure 1: Exo-101's immunomodulatory effects *in vitro*. (**a-f**) THP-1-derived macrophages, with or without LPS stimulation as indicated, were incubated with 1×10^{10} particles/mL of Exo-101 for 24h, before flow cytometry analysis ($n \geq 3$). (**g-j**) Relative expression of M1-associated genes by qPCR ($n \geq 3$) and (**k, l**) release of pro-inflammatory molecules by ELISA ($n \geq 6$). (**m, n**) Proliferation of normal human dermal fibroblasts, 2 and 6 days after incubation with Exo-101 (1×10^{10} particles/mL) or media of Exo-101-stimulated macrophages ($n \geq 6$), and (**o**) CXCL8 expression at 48h ($n \geq 3$). (**p-u**) Human PBMC, stimulated with PMA or

αCD3/αCD28 as indicated, were incubated with a single dose of Exo-101 at $1x10^{10}$ particles/mL for 6 days, followed by flow cytometry analysis (n≥3). (**v, w**) TNFα and CCL20 release by LPS-stimulated PBMC after a 24h incubation with $1x10^{10}$ particles/mL Exo-101 (n=3). (**x-aa**) Relative expression of transcription factors by PBMC incubated with Exo-101 for 2 or 6 days (n≥3). Cells were sorted based on FSC, SSC, CD3 and CD4, prior to RNA extraction. (**ab-ad**) Phenotyping of αCD3/αCD28-activated PBMC, after 6 days of incubation with Exo-101 at $1x10^{10}$ particles/mL or IL-2 (100 IU/ml) and TGF-β (5ng/mL) (n=6). All results are presented as mean +/- SD. *p≤0.05, **p≤0.01, ***p≤0.001, ****p≤0.0001. NS, non-stimulated; NT, non-treated; CM, conditioned media.

Figure 2: Decreased expression of epidermal psoriatic features after Exo-101 treatment. Relative expression of (**a-h**) pro-inflammatory mediators and (**i, j**) anti-microbial peptides by a 3D model of human psoriatic epidermis, treated with $1x10^{10}$ particles/mL Exo-101 twice daily for 6 days (n=3). All results are presented as mean +/- SD. *p≤0.05, **p≤0.01.

Figure 3: Therapeutic potential of Exo-101 for imiquimod-induced psoriasis. C57BL/6 mice received 5% imiquimod (IMQ) on their shaved backs (approx. 7 cm^2), daily for 6 days. A topical formulation containing $2x10^{10}$ particles/mL Exo-101 was applied to the same area every day, 1h after IMQ. (**a**) Representative photos and (**b**) clinical score (n=6). (**c**) Representative H&E microphotographs used to measure (**d**) epidermal thickness (n≥4). Scale bars=250μm or 100μm, respectively for upper and lower microphotographs. Epidermal thickness was measured from *stratum basale* to *stratum granulosum*, averaging 5 measurements per section, for a total of 20 data points per animal. (**e-i**) Relative expression of pro-inflammatory mediators in the skin of all tested groups (n≥4). (**j-m**) Digested skin of all

four test groups was analyzed by flow cytometry for identification of total, $CD4^+$, $CD8^+$ and regulatory T-cells (n≥2). All results are presented as mean +/- SD. *p≤0.05, **p≤0.01.

Figure S1: Effects of Exo-101 treatment on gene expression of chronic skin wounds. STZ-induced diabetic mice were treated topically with 2.5×10^9 particles/mL Exo-101, twice per day for 15 days, after which skin mRNA was extracted. The inverted triangle on the left represents the different major processes affected by Exo-101 treatment. The circles on the right illustrate the percentage of inflammation- and immune system-related genes up- or down-regulated after Exo-101 treatment.

Figure S2: Effects of Exo-101 treatment on the percentage of regulatory T-cells (Treg). Human PBMC were activated with αCD3/αCD28 and treated for 6 days with Exo-101 (1×10^{10} particles/mL) or IL-2 (100 IU/ml) and TGF-β (5ng/mL) (n=6). Treg were defined as $CD3^+CD4^+CD25^+FOXP3^+$ cells. Comparison with Figure 1ab, where Treg were identified based on the expression markers CD25 and CD127. All results are presented as mean +/- SD. **p≤0.01. NT, non-treated.

Figure S3: Cell populations in the skin of imiquimod- and Exo-101 treated animals. Flow cytometry identification of neutrophils, γδ T-cells and macrophages in digested skin of mice treated with imiquimod (IMQ) and/or Exo-101 as indicated (n≥2). All results are presented as mean +/- SD.

Figure S4: FOXP3 expression in the skin of Exo-101 treated mice with chronic wounds. STZ-induced diabetic mice (n=4) were treated topically with 2.5×10^9 particles/mL Exo-101 or

vehicle, twice per day for 15 days, after which skin mRNA was extracted. All results are
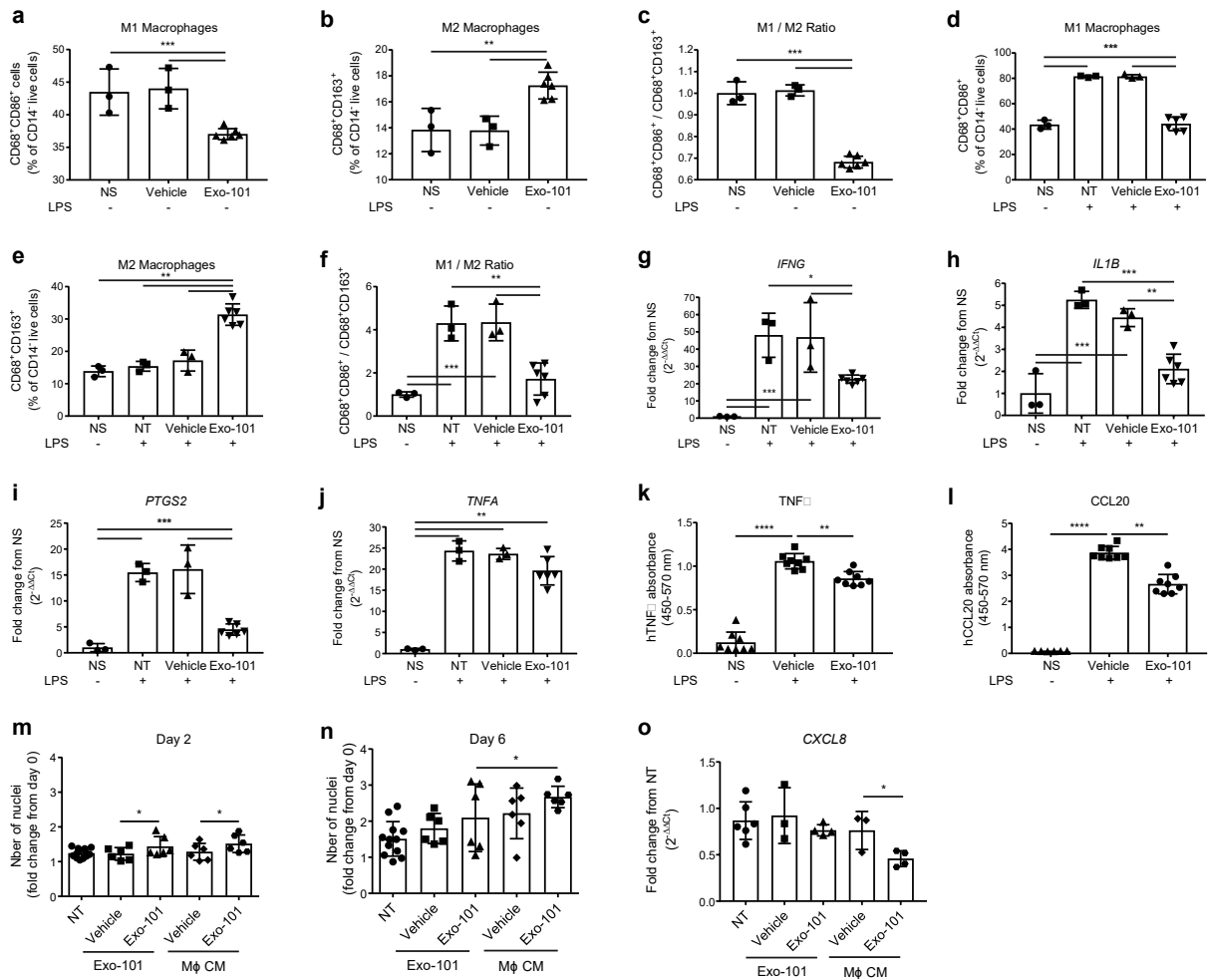
presented as mean +/- SD. *p≤0.05.

Figure 1: Exo-101's modulatory effects on macrophages and fibroblasts *in vitro*. (**a-f**) THP-1-derived macrophages, with or without LPS stimulation as indicated, were incubated with $1x10^{10}$ particles/mL of Exo-101 for 24h, before flow cytometry analysis (n≥3). (**g-j**) Relative expression of M1-associated genes by qPCR (n≥3) and (**k, l**) release of pro-inflammatory molecules by ELISA (n≥6). (**m, n**) Proliferation of normal human dermal fibroblasts, 2 and 6 days after incubation with Exo-101 ($1x10^{10}$ particles/mL) or media of Exo-101-stimulated macrophages (n≥6), and (**o**) CXCL8 expression at 48h (n≥3). All results are presented as mean +/- SD. *p≤0.05, **p≤0.01, ***p≤0.001, ****p≤0.0001. NS, non-stimulated; NT, non-treated; CM, conditioned media.
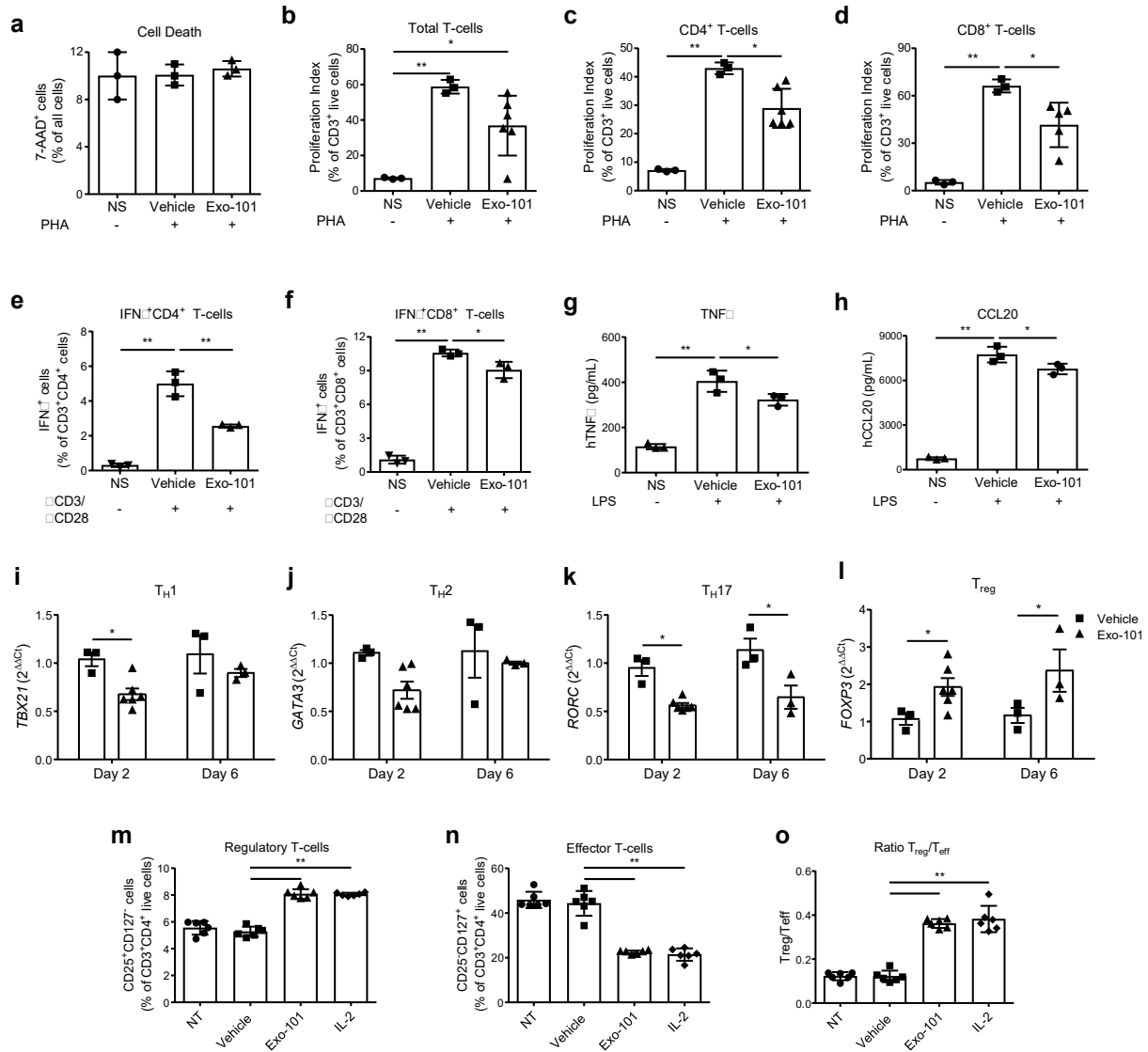
Figure 2: Exo-101's immunomodulatory effects on T-cells *in vitro*. (**a-f**) Human PBMC, stimulated with PMA or αCD3/αCD28 as indicated, were incubated with a single dose of Exo-101 at 1×10^{10} particles/mL for 6 days, followed by flow cytometry analysis (n≥3). (**g, h**) TNFα and CCL20 release by LPS-stimulated PBMC after a 24h incubation with 1×10^{10} particles/mL Exo-101 (n=3). (**i-l**) Relative expression of transcription factors by PBMC incubated with Exo-101 for 2 or 6 days (n≥3). Cells were sorted based on FSC, SSC, CD3 and CD4, prior to RNA extraction. (**m-o**) Phenotyping of αCD3/αCD28-activated PBMC, after 6 days of incubation with Exo-101 at 1×10^{10} particles/mL or IL-2 (100 IU/ml) and TGF-β (5ng/mL) (n=6). All

results are presented as mean +/- SD. *p≤0.05, **p≤0.01, ***p≤0.001, ****p≤0.0001. NS,

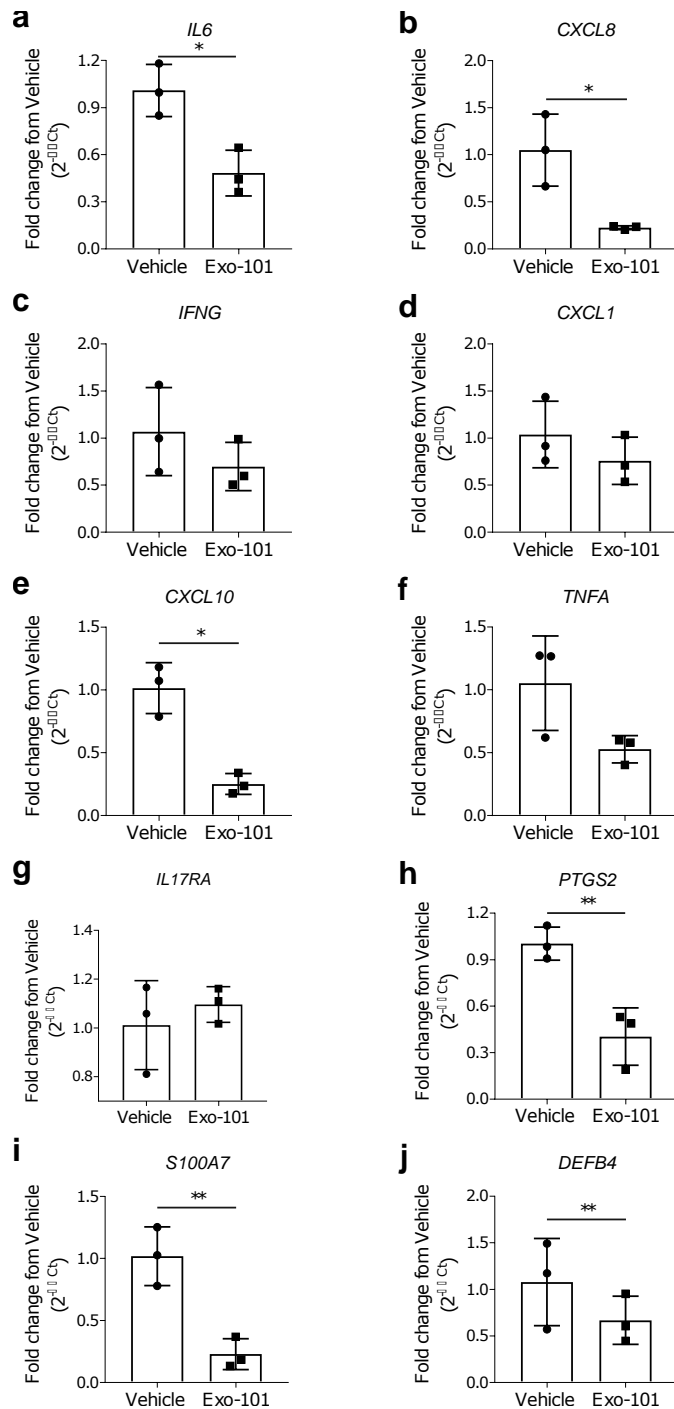non-stimulated; NT, non-treated.

Figure 3: Decreased expression of epidermal psoriatic features after Exo-101 treatment.

Relative expression of (**a-h**) pro-inflammatory mediators and (**i, j**) anti-microbial peptides by a 3D model of human psoriatic epidermis, treated with 1×10^{10} particles/mL Exo-101 twice daily for 6 days (n=3). All results are presented as mean +/- SD. $*p \leq 0.05$, $**p \leq 0.01$.
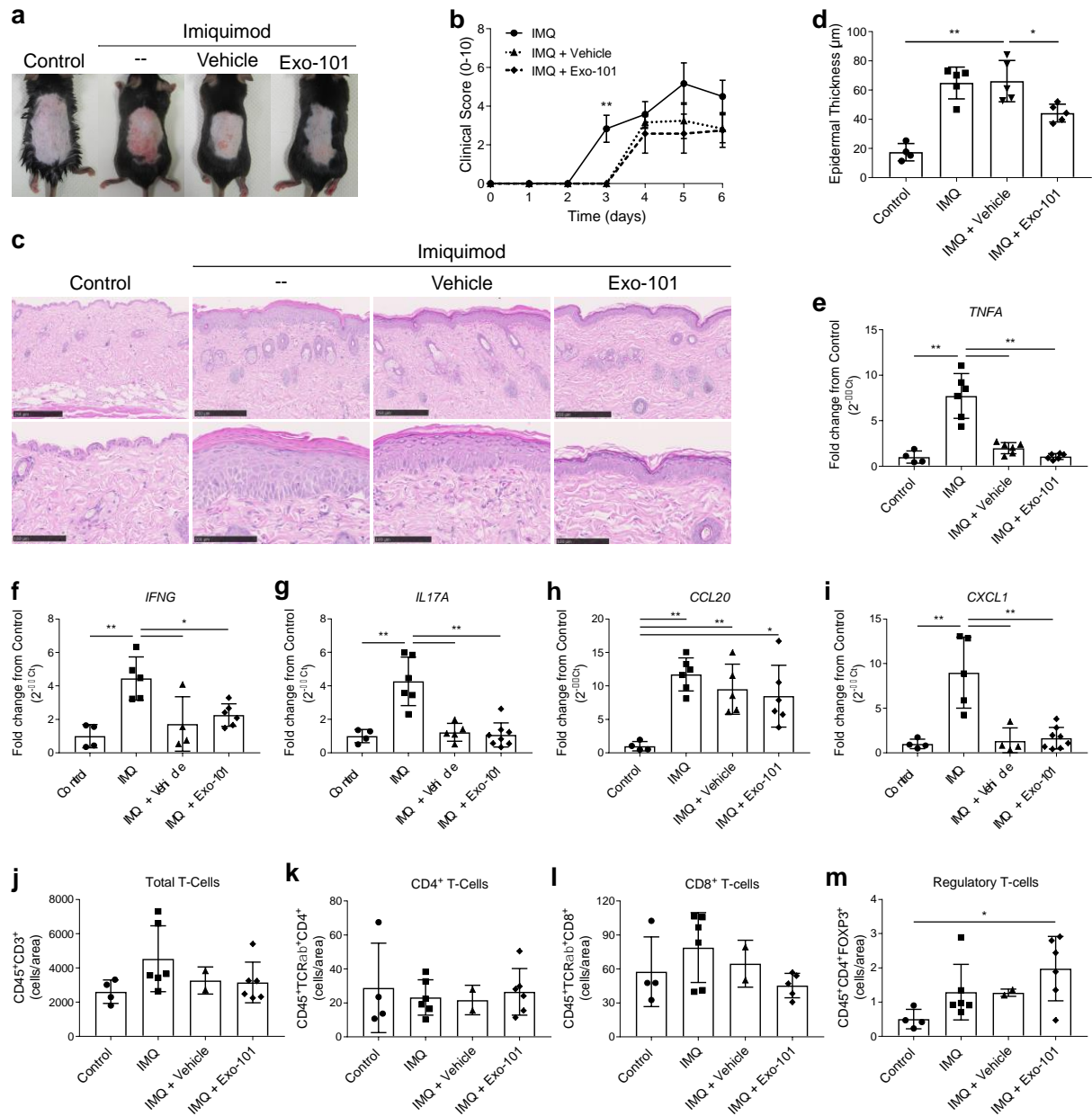
Figure 4: Therapeutic potential of Exo-101 for imiquimod-induced psoriasis. C57BL/6 mice received 5% imiquimod (IMQ) on their shaved backs (approx. 7 cm^2), daily for 6 days. A topical formulation containing 2×10^{10} particles/mL Exo-101 was applied to the same area every day, 1h after IMQ. (**a**) Representative photos and (**b**) clinical score (n=6). (**c**) Representative H&E microphotographs used to measure (**d**) epidermal thickness (n≥4). Scale bars=250μm or 100μm, respectively for upper and lower microphotographs. Epidermal thickness was measured from *stratum basale* to *stratum granulosum*, averaging 5

measurements per section, for a total of 20 data points per animal. (**e-i**) Relative expression of pro-inflammatory mediators in the skin of all tested groups (n$\geq$4). (**j-m**) Digested skin of all four test groups was analyzed by flow cytometry for identification of total, CD4$^+$, CD8$^+$ and regulatory T-cells (n$\geq$2). All results are presented as mean +/- SD. *p$\leq$0.05, **p$\leq$0.01.
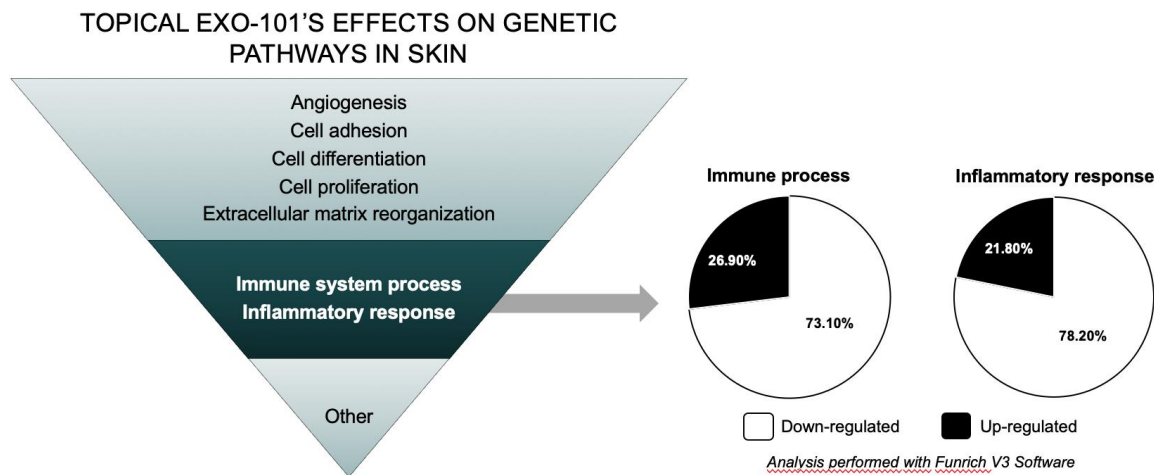
Figure S1: Effects of Exo-101 treatment on gene expression of chronic skin wounds.

STZ-induced diabetic mice were treated topically with 2.5×10^9 particles/mL Exo-101, twice per day for 15 days, after which skin mRNA was extracted. The inverted triangle on the left represents the different major processes affected by Exo-101 treatment. The circles on the right illustrate the percentage of inflammation- and immune system-related genes up- or down-regulated after Exo-101 treatment.
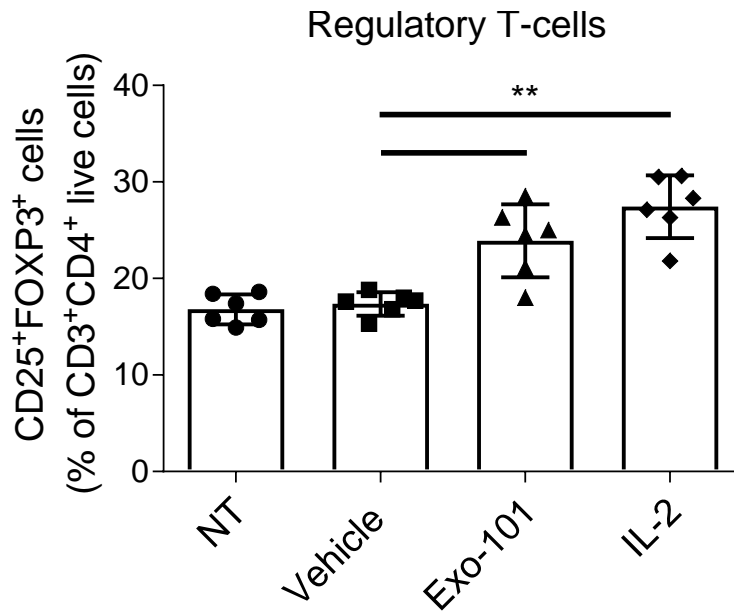
Figure S2: Effects of Exo-101 treatment on the percentage of regulatory T-cells (Treg).

Human PBMC were activated with αCD3/αCD28 and treated for 6 days with Exo-101 ($1x10^{10}$ particles/mL) or IL-2 (100 IU/ml) and TGF-β (5ng/mL) (n=6). Treg were defined as $CD3^+CD4^+CD25^+FOXP3^+$ cells. Comparison with Figure 1ab, where Treg were identified based on the expression markers CD25 and CD127. All results are presented as mean +/- SD. **$p \leq 0.01$. NT, non-treated.
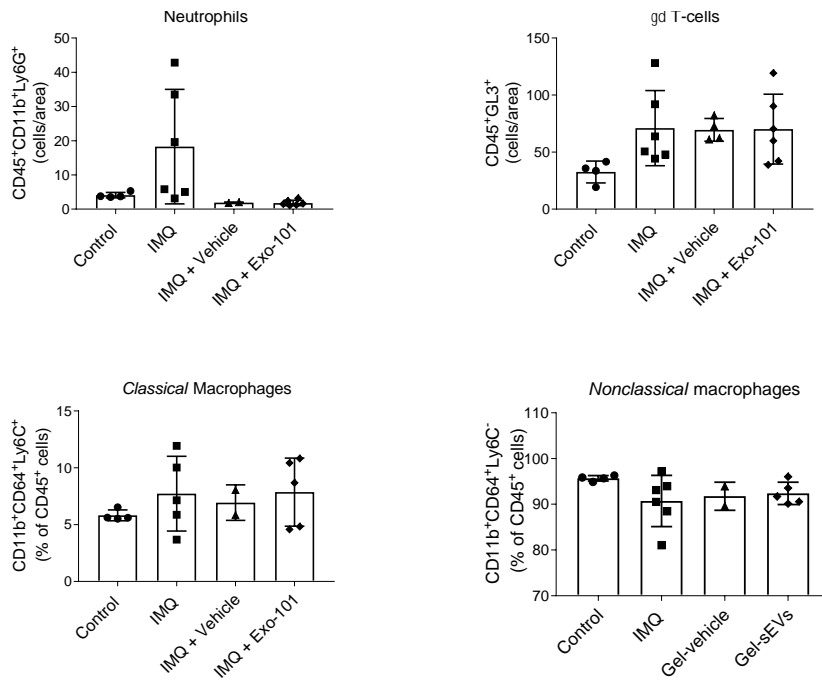
Figure S3: Cell populations in the skin of imiquimod- and Exo-101 treated animals. Flow cytometry identification of neutrophils, γδ T-cells and macrophages in digested skin of mice treated with imiquimod (IMQ) and/or Exo-101 as indicated (n≥2). All results are presented as mean +/- SD.
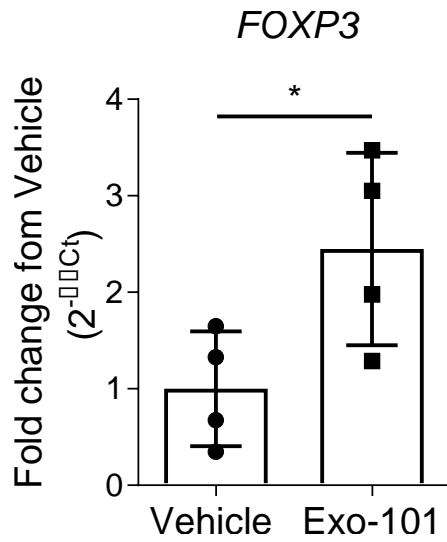
Figure S4: FOXP3 expression in the skin of Exo-101 treated mice with chronic wounds.

STZ-induced diabetic mice (n=4) were treated topically with 2.5×10^9 particles/mL Exo-101 or vehicle, twice per day for 15 days, after which skin mRNA was extracted. All results are presented as mean +/- SD. *p$\leq$0.05.